Impact of van der Waals Interactions on Single Asperity Friction

Matthias Lessel,[1] Peter Loskill,[1] Florian Hausen,[2] Nitya Nand Gosvami,[2] Roland Bennewitz,[2] and Karin Jacobs[1,*]

[1]*Department of Experimental Physics, Saarland University, D-66123 Saarbrücken, Germany*

[2]*INM Leibniz-Institute for New Materials, D-66123 Saarbrücken, Germany*

(Received 4 March 2013; published 16 July 2013)

Single asperity measurements on Si wafers with variable SiO_2 layer thickness, yet identical roughness, revealed the influence of van der Waals (vdW) interactions on friction: on thin (1 nm) SiO_2 layers, higher friction and jump-off forces were observed as compared to thick (150 nm) SiO_2 layers. The vdW interactions were additionally controlled by a set of silanized Si wafers, exhibiting the same trend. The experimental results demonstrate the influence of the subsurface material and are quantitatively described by combining calculations of interactions of the involved materials and the Derjaguin-Müller-Toporov model.

DOI: 10.1103/PhysRevLett.111.035502 PACS numbers: 81.40.Pq, 07.79.Sp, 46.55.+d, 68.35.Np

Understanding friction plays a key role for the design of modern micro- and nanomechanical devices. Towards smaller scales, the surface to volume ratio increases and surface-related phenomena start playing a dominant role. Scanning probe microscopy (SPM) is a common tool to study single asperity contact mechanics.

Numerous previous nanoscale friction studies probed multiple surface properties such as roughness, surface energy, surface chemistry, or crystal order of the substrate, the results of which are compiled in recent reviews (see, e.g., Refs. [1–4] and references therein).

An aspect frequently neglected is van der Waals–Casimir interactions. Of quantum mechanical origin, these dipole-dipole interactions are present at every interface and are one summand in the effective interface potential (or interaction potential) of the involved materials. This aspect is not only of fundamental interest to understand friction, it is also important for surface-related applications: for micromachined surfaces, the importance of van der Waals (vdW) interactions was highlighted only in the last two decades [5,6]; also the stability of coatings is affected [7,8] as well as the adhesion forces of bacteria to, e.g., functionalized surfaces [9]. These studies varied the subsurface composition of the materials to tune the vdW interactions. Thereby, a variation in the interaction energy can be achieved [10–13], which is sufficient to induce significant differences in adhesion forces even for macroscopic objects such as geckos [14].

This work presents a unique direct demonstration that friction is not only influenced by surface properties (e.g., roughness, surface chemistry, and surface energy), but also by the composition of the substrate in the subsurface regime. Theoretical calculations employing the determination of vdW forces and the contact mechanics model of Derjaguin-Müller-Toporov capture the experimental findings quantitatively.

In this Letter, we report on single asperity friction experiments on stratified Si substrates. The substrates consist of Si wafers covered with SiO_2 layers of different thickness [*N* (native) for 0.9 nm SiO_2 and *T* (thick) for 150 nm SiO_2]. To rule out the effects of surface chemistry and surface energy, we hydrophobized both types of substrate by employing an octadecyl-trichlorosilane (OTS) self-assembled monolayer (SAM) [15] (*N-hydrophob* for OTS with 0.9 nm SiO_2 and *T-hydrophob* for OTS on 150 nm SiO_2). The SAMs are densely packed and exhibit a nearly crystalline structure [15,16] (see Supplemental Material [17]). Moreover, the *T*-type substrates feature the same high quality of the silane SAMs as the *N*-type surfaces. The calculated number of silane chains per square area is 4.5 chains/nm^2 indicating an optimal silane density [18]. Each (*N*, *T*) pair of the different surface types (*hydrophil* and *hydrophob*) provides the same surface chemistry, energy, and roughness and differs only in the subsurface composition (i.e., the thickness of the SiO_2 layer) (cf. Table I). A detailed analysis of the roughness of the SiO_2 substrates utilizing Minkowski functionals can be found in the Supplemental Material [17]. The results of this analysis show that the SiO_2 surfaces (*N* and *T*) can be treated as random Gaussian surfaces.

The friction and jump-off forces determined on both pairs of substrates, however, show significant differences (cf. Fig. 1). Thereby, *N*-type substrates exhibit higher jump-off and friction forces than *T*-type substrates. These differences must be due to the different subsurface compositions and thereby induced variations in the vdW interactions [12,15]. In other words, the vdW interactions seems to contribute to friction like an additional normal force. Since *N*- and *T-hydrophil* as well as *N*- and *T-hydrophob* substrates feature the same surface chemistry and structure, a change of a fundamental dissipation mechanism concerning friction is not expected.

The experiments were performed with Si_3N_4 tips (DNP-S, Bruker AFM Probes, Camarillo, CA, USA) with a nominal tip radius of 10 nm. The tips were blunted following a procedure described by Maw *et al.* [19] in

TABLE I. Surface properties of the studied substrates (taken from Ref. [15]; see also the Supplemental Material [17]).

Subtrate type	SiO_2 thickness [nm]	OTS thickness [nm]	Roughness [nm] (rms on 1 μm^2)	H_2O contact angle (advancing)	Surface energy [mJ/m^2]
N-hydrophil	0.9	···	0.09(2)	7(2)°	63(1)
T-hydrophil	150	···	0.13(2)	5(2)°	64(1)
N-hydrophob	0.9	2.8	0.12(2)	111(2)°	24(1)
T-hydrophob	150	2.8	0.15(2)	110(2)°	24(1)

order to increase the overall friction force (cf. Fig. 2). Also, the blunting leads to a very high reproducibility of the measured friction forces vs applied load. To accomplish the blunting, the probes were scanned with a Catalyst SPM (Bruker Nano Inc., Santa Barbara, CA, USA) in contact mode in de-ionized water on a *N-hydrophil* wafer with a tip velocity of 16 μm/s for 120 min with an applied load of 50 nN. Subsequently, the spring constants were derived using the method described by Sader *et al.* [20,21].

All friction experiments were performed under standard lab conditions (25 °C, approximately 50% humidity). Prior to friction measurements, the surface was examined for surface defects or contaminations. After the experiments, the surface was examined again to exclude any damage and wear. Neither of the two were observed during the experiments [17]. Also, measurements on different surface spots on the same substrate showed no differences in friction force.

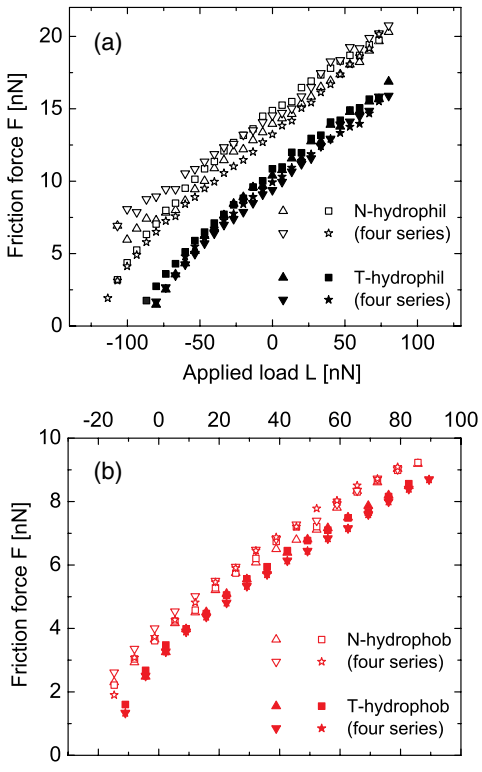

FIG. 1 (color online). Friction vs applied load on (a) hydrophilic (*N-hydrophil* and *T-hydrophil*) and (b) hydrophobic (*N-hydrophob* and *T-hydrophob*) substrates.

The friction experiments were performed using a SPM (Agilent 5500, Agilent Technologies, Santa Clara, CA, USA) in contact mode. Data were recorded with 4.8 Hz and 128×128 pixels resolution for a scan area of $(500\ nm)^2$. From the 128×128 pixels per image only 96×96 pixels from the center part of the image were used to calculate the friction force in order to rule out edge effects.

The same tip was used to measure *N*- and *T*-type substrates. On every surface, two spots were probed and for each spot a cycle of increasing and decreasing load—ranging from 80 nN to lift off—was recorded. Before and after every load cycle, force distance measurements were taken to check for tip changes and to calibrate the zero load value of the SPM. Thereby, any effect of thermal drift can be ruled out.

In contrast to previous studies [22], we did not observe superlinear behavior for friction forces on OTS covered substrates. This difference can be attributed to a homogeneous and highly ordered silane SAM [15] and also. on the other hand, to a much larger tip curvature used for this study.

To recapitulate, the experimental jump-off and friction forces differ depending on the surface chemistry (*hydrophil* and *hydrophob*) as expected from the literature. Moreover, our experiments reveal a difference in jump-off and friction forces on substrates with identical surface properties but different thicknesses of the SiO_2 layers. This difference was observed independently of the respective surface chemistry.

Since the surface characteristics such as roughness, surface energy, and water contact angles are identical within the experimental error (cf. Table I), the force differences cannot be caused by capillary or roughness effects

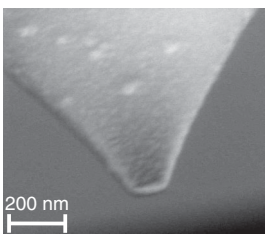

FIG. 2. Scanning electron micrograph of a blunted tip.

or the stoichiometry of the SiO_2 [17]. Furthermore, an effect of different elastic moduli for N- and T-type substrates can also be ruled out: though the overall elastic moduli of the N-type substrates could be higher compared to the T-type substrates due to the smaller distance to the underlying harder Si [23,24], it would only induce a load-dependent effect and could not explain the observed differences in jump-off and friction forces.

Electrostatic effects can also be ruled out as an origin for the observed differences: a signature of electrostatic forces is very high jump-off forces, which were not observed during the experiments. Moreover, since the experiments were performed in standard atmosphere, surface charges should be dissipated. Another aspect to consider is tribo-electrification of the tip and surface, which could also contribute to friction [25]. Upon separation of a contact (here by continuing sliding) a charge may be transferred from the tip to the sample. However, high quality SAMs are very unlikely charge traps, and so are thick oxides. If there was significant charging, enormous jump-off forces would result, which are not observed as mentioned above.

Both effects—the increase in jump-off and friction forces on the N-type substrates compared to the T-type ones—can be explained by considering different van der Waals interactions between the probe and N- and T-type substrates. Since vdW interactions depend on the volume properties of the substrate, they are influenced by the subsurface composition—viz., the thickness of the oxide layers. Qualitatively, the higher polarizability of silicon compared to silicon dioxide induces a stronger interaction between the probe and the N-type substrate than with the T type, which is in agreement with the experimental findings (cf. Fig. 1).

To compare the experimental results with theoretical predictions, we applied the Derjaguin-Müller-Toporov (DMT) model [26] to the friction data. The DMT model is appropriate due to the involved relatively weak forces and stiff materials. This assumption is corroborated by the respective Maugis parameters $\lambda^{T\text{-hydrophil}} \approx 0.04$ and $\lambda^{T\text{-hydrophob}} \approx 0.006$ (DMT regime $\lambda < 0.1$) [27,28]. An extraordinarily good agreement is found between the experimental data and the DMT model fit $[F \propto (L - L_{\text{jump-off}})^{(2/3)}]$ for all probed surface types [cf. Figs. 3(a) and 3(b)].

For the experiments on the hydrophilic samples, the fits yield the jump-off force of $L_{\text{jump-off}}^{N\text{-hydrophil}} = -124(2)$ nN and $L_{\text{jump-off}}^{T\text{-hydrophil}} = -85.5(5)$ nN.

The fit produces reasonable system parameters (mean curvature $\kappa^{\text{hydrophil}} = 0.110(2)\ \mu\text{m}^{-1}$, normalized shear strength $\tau^*_{N\text{-hydrophil}} = 0.420(6)\ \text{Pa}^{1/3}$ and $\tau^*_{T\text{-hydrophil}} = 0.387(2)\ \text{Pa}^{1/3}$; for further details see the Supplemental Material [17]). In the case of the hydrophobic samples, we obtain jump-off forces of $L_{\text{jump-off}}^{N\text{-hydrophob}} = -30.4(8)$ nN and $L_{\text{jump-off}}^{T\text{-hydrophob}} = -23.8(5)$ nN. Again, reasonable system parameters (mean curvature $\kappa^{\text{hydrophob}} = 0.053(1)\ \mu\text{m}^{-1}$, normalized shear strength $\tau^*_{N\text{-hydrophob}} = 0.177(3)\ \text{Pa}^{1/3}$ and $\tau^*_{T\text{-hydrophob}} = 0.169(3)\ \text{Pa}^{1/3}$) result from the fit.

To allow a quantitative prediction, however, the next step is to calculate the effective interface potentials for N- and T-type systems. Considering two semi-infinite half slabs [29] of materials i and j interacting through a

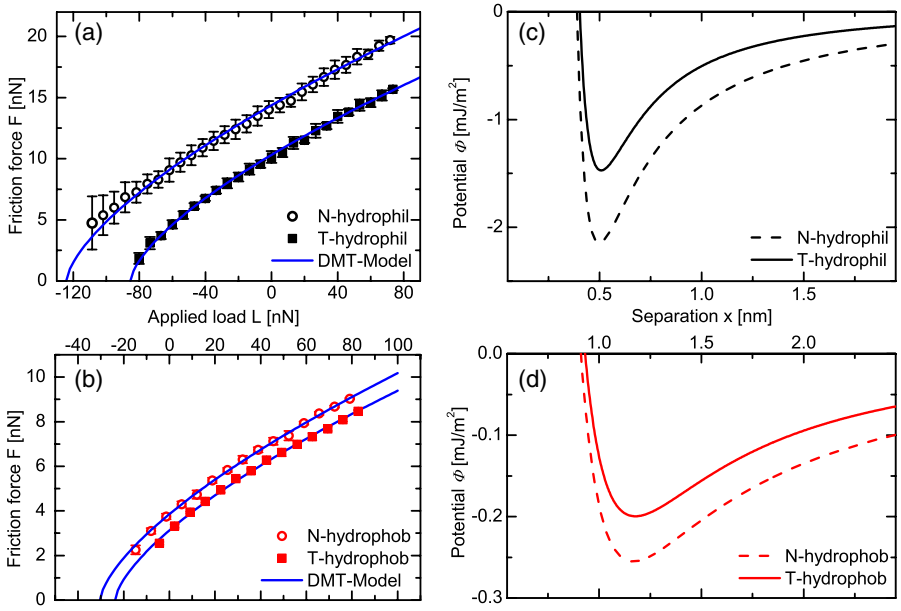

FIG. 3 (color online). (a), (b) Mean values of friction data vs applied load on hydrophilic (a) and hydrophobic (b) substrates and respective theoretical predictions using the DMT model. For most of the data points, the error bar is smaller than the symbol size. (c), (d) Calculated effective interface potentials for the hydrophilic (c) and hydrophobic (d) systems.

TABLE II. Hamaker constants[a] for the interactions of silicon nitride with various materials through water[b]. Dielectrical data of decane are the closest representation for the OTS-SAM.

Material 3 (M3)	$A_{Si_3N_4/H_2O/M3}$ [zJ]
silicon	68.7
silica	19.1
decane (OTS)	13

[a]Constants are calculated using the Ninham-Parsegian representation [32].
[b]As medium M, water is employed, since all surfaces are covered by a water layer at ambient conditions [34].

medium M, the nonretarded [30] interaction energy per unit area is given by $\phi_{\mathrm{vdW}}(x) = -A_{i/M/j}/(12\pi x^2)$ with the Hamaker constant $A_{i/M/j}$. In the case of one single layered sample, the nonretarded interaction energy per unit area can be approximated by Refs. [8,31], which is directly based on the Lifshitz theory:

$$\phi_{\mathrm{vdW}}(x) = -\frac{1}{12\pi}\left[\frac{A_{i/M/l}}{x^2} + \frac{A_{i/M/l} - A_{i/M/j}}{(x+d)^2}\right], \quad (1)$$

whereby the probe object is of uniform material i and the substrate is composed of material j and coated with a layer of material l and thickness d. In this study, the respective Hamaker constants for the involved materials were calculated by employing the Ninham-Parsegian representation [32] of the $\varepsilon(i\zeta)$ functions as described in Ref. [33]. The values listed in Table II are calculated using dielectrical data for decane from Ref. [35], for water from Ref. [36], and for silicon, silica, and silicon nitride from Ref. [37].

The vdW interactions are only one part of the effective interface potential. To account for short-range interactions, an additional term $\phi_{\mathrm{SR}}(x) = C_{\mathrm{SR}}/x^m$ has to be added to the interface potential. By choosing $m = 8$, the difference in the exponents within the classical Lennard-Jones potential is preserved. Unfortunately, it is not possible to predict theoretically the values of the short-range constants C_{SR} due to the lack of a direct physical access. However, since the short-range interactions are determined solely by the topmost atomic layer, they are identical for the N- and T-type substrates featuring the same surface chemistry, also indicated by identical values of the water contact angle (cf. Table I). Hence, it is plausible to obtain the respective constants directly from the experimental data, i.e., the jump-off forces.

According to the DMT model, the jump-off forces solely depend on the curvature of the tip and the work of adhesion $\gamma^{N,T}$; the latter can be linked to the global minimum $\phi^{N,T}_{\mathrm{min}}$ of the effective interface potential [14]:

$$L^{N,T}_{\mathrm{jump\text{-}off}} = -\frac{2\pi}{\kappa}\gamma^{N,T} = -\frac{2\pi}{\kappa}\phi^{N,T}_{\mathrm{min}}. \quad (2)$$

Since the identical SPM tip (hence the same curvature) was used on N- and T-type substrates (*hydrophil* and *hydrophob*), the ratios of the jump-off forces can be employed to gain the unknown short-range constants. By this, we obtain $C_{\mathrm{SR}}^{\mathrm{hydrophob}} = 2.34 \times 10^{-76}\ \mathrm{J\,m^2}$ and $C_{\mathrm{SR}}^{\mathrm{hydrophil}} = 2.1 \times 10^{-78}\ \mathrm{J\,m^2}$ leading to the respective interface potentials, as depicted in Figs. 3(c) and 3(d).

In other words, the differences in jump-off and friction forces observed in the experiments can be correlated to the different effective interface potentials for N- and T-type substrates. Except for the small difference in distance between the AFM tip and the SiO_2/Si interface for both the bare and the SAM-covered surfaces (2.8 nm), the van der Waals contribution is the same for hydrophobic and hydrophilic termination of the surface, as shown by the same relative increase in the jump-off and friction forces in each case.

To conclude, the influence of van der Waals interactions on the single asperity friction on hydrophilic and hydrophobic substrates is demonstrated. The van der Waals interactions are tuned by varying the oxide layer thickness of the substrates. The jump-off and friction forces are stronger on the substrates with a thin oxide layer than on substrates with a thick oxide layer independently of the surface energy and roughness. For both types of surfaces (hydrophilic and hydrophobic), the experimental data can be described by theoretical calculations of the effective interface potentials in combination with the DMT model. The results demonstrate that van der Waals contributions have to be considered in order to quantitatively describe friction forces; this requires a thorough understanding of the composition of the interacting objects.

Authors at the Saarland University acknowledge support from the Deutsche Forschungsgemeinschaft (DFG) as part of the Priority Program SPP 1164 and the graduate college GRK 1276. Authors at the INM acknowledge support from the DFG as part of the ESF EUROCORES Programme and thank Eduard Arzt for continuing support on this study.

*k.jacobs@physik.uni-saarland.de

[1] M. Nosonovsky and B. Bhushan, Mater. Sci. Eng. R **58**, 162 (2007).
[2] I. Szlufarska, C. Michael, and R. W. Carpick, J. Phys. D **41**, 123001 (2008).
[3] J. Krim, Adv. Phys. **61**, 155 (2012).
[4] A. Vanossi, N. Manini, M. Urbakh, S. Zapperi, and E. Tosatti, Rev. Mod. Phys. **85**, 529 (2013).
[5] F. W. Delrio, M. P. De Boer, J. A. Knapp, E. D. Reedy, Jr., P. J. Clews, and M. L. Dunn, Nat. Mater. **4**, 629 (2005).
[6] F. M. Serry, D. Walliser, and G. J. Maclay, J. Appl. Phys. **84**, 2501 (1998).
[7] R. Seemann, S. Herminghaus, C. Neto, S. Schlagowski, D. Podzimek, R. Konrad, H. Manz, and K. Jacobs, J. Phys. Condens. Matter **17**, S267 (2005).
[8] R. Seemann, S. Herminghaus, and K. Jacobs, Phys. Rev. Lett. **86**, 5534 (2001).

[9] P. Loskill, H. Hähl, N. Thewes, C. T. Kreis, M. Bischoff, M. Herrmann, and K. Jacobs, Langmuir **28**, 7242 (2012).
[10] R. Podgornik and V. A. Parsegian, J. Chem. Phys. **120**, 3401 (2004).
[11] J. Rafiee, X. Mi, H. Gullapalli, A. V. Thomas, F. Yavari, Y. Shi, P. M. Ajayan, and N. A. Koratkar, Nat. Mater. **11**, 217 (2012).
[12] P. Loskill, H. Hähl, T. Faidt, S. Grandthyll, F. Müller, and K. Jacobs, Adv. Colloid Interface Sci. **179–182**, 107 (2012).
[13] R. B. Walsh, A. Nelson, W. M. Skinner, D. Parsons, and V. S. J. Craig, J. Phys. Chem. C **116**, 7838 (2012).
[14] P. Loskill, J. B. Puthoff, M. Wilkinson, K. Mecke, K. Jacobs, and K. Autumn, J. R. Soc. Interface **10**, 20120587 (2012).
[15] M. Lessel, O. Bäumchen, R. Fetzer, M. Klos, H. Hähl, R. Seemann, and K. Jacobs, http://arxiv.org/abs/1212.0998.
[16] H. Hähl, F. Evers, S. Grandthyll, M. Paulus, C. Sternemann, P. Loskill, M. Lessel, A. K. Hüsecken, T. Brenner, M. Tolan *et al.*, Langmuir **28**, 7747 (2012).
[17] See Supplemental Material at http://link.aps.org/supplemental/10.1103/PhysRevLett.111.035502 for a detailed roughness analysis of the Si wafers, a structural analysis of silane SAMs by X-ray reflectometry, and the calculation of the normalized shear strength.
[18] B. W. Ewers and J. D. Batteas, J. Phys. Chem. C **116**, 25 165 (2012).
[19] W. Maw, F. Stevens, S. C. Langford, and J. T. Dickinson, J. Appl. Phys. **92**, 5103 (2002).
[20] J. E. Sader, I. Larson, P. Mulvaney, and L. R. White, Rev. Sci. Instrum. **66**, 3789 (1995).
[21] C. P. Green, H. Lioe, J. P. Cleveland, R. Proksch, P. Mulvany, and J. E. Sader, Rev. Sci. Instrum. **75**, 1988 (2004).
[22] E. E. Flater, W. R. Ashurst, and R. W. Carpick, Langmuir **23**, 9242 (2007).
[23] B. Bhushan and X. Li, J. Mater Res. **12**, 54 (1997).
[24] M. T. Kim, Thin Solid Films **283**, 12 (1996).
[25] I. Altfeder and J. Krim, J. Appl. Phys. **111**, 094916 (2012).
[26] B. V. Derjaguin, V. M. Muller, and Y. P. Toporov, J. Colloid Interface Sci. **53**, 314 (1975).
[27] D. Maugis, J. Colloid Interface Sci. **150**, 243 (1992).
[28] R. W. Carpick, D. F. Ogletree, and M. Salmeron, J. Colloid Interface Sci. **211**, 395 (1999).
[29] This assumption seems appropriate due to the very low curvature of the blunted tips.
[30] Retardation effects can be neglected on these small tip-surface separations. See J. N. Israelachvili, and D. Tabor, Nature (London) **236**, 106 (1972).
[31] The identical results were obtained when using Eq. L1.25 from V. A. Parsegian, *Van der Waals Forces: A Handbook for Biologists, Chemists, Engineers, and Physicists* (Cambridge University Press, Cambridge, England, 2006), 1st ed.
[32] V. A. Parsegian and B. W. Ninham, Nature (London) **224**, 1197 (1969).
[33] D. B. Hough and L. R. White, Adv. Colloid Interface Sci. **14**, 3 (1980).
[34] D. B. Asay and S. H. Kim, J. Chem. Phys. **124**, 174712 (2006).
[35] T. Masuda, Y. Matsuki, and T. Shimoda, J. Colloid Interface Sci. **340**, 298 (2009).
[36] V. A. Parsegian and G. H. Weiss, J. Colloid Interface Sci. **81**, 285 (1981).
[37] T. J. Senden and C. J. Drummond, Colloids Surf. A **94**, 29 (1995).